

Valence and spin state of Co and Ni ions and their relation to metallicity and ferromagnetism in $\text{LaCo}_{0.5}\text{Ni}_{0.5}\text{O}_3$

Tôru Kyômen, Ryutarô Yamazaki, and Mitsuru Itoh*

Materials and Structures Laboratory, Tokyo Institute of Technology, 4259 Nagatsuta, Midori-ku, Yokohama 226-8503, Japan

(Received 13 January 2003; revised manuscript received 14 April 2003; published 17 September 2003)

$\text{LaNi}_{0.5}\text{Co}_{0.5}\text{O}_3$ was measured in terms of x-ray-absorption near-edge structure (XANES), powder x-ray diffraction, magnetic susceptibility, resistivity, and heat capacity. A small but clear heat capacity anomaly and an ac susceptibility peak were observed at 53 K. The peak temperature and magnitude of the ac susceptibility were found to be, respectively, independent of and dependent on frequency. The magnetization reversal at the coercive force is sharp but the magnetization does not saturate even at 50 kOe and 5 K. The resistivity is on the order of $10^{-3} \Omega \text{ cm}$ and the contribution from conductive electrons to the heat capacity was observed at low temperatures. These results are consistent with the earlier conclusion that $\text{LaCo}_{0.5}\text{Ni}_{0.5}\text{O}_3$ is a metallic ferromagnet with a certain disorder with respect to magnetic interaction. XANES indicated that both valences of Co and Ni ions are trivalent. The unit-cell volume is larger than that of either LaCoO_3 or LaNiO_3 below room temperature, which suggests that the population of Co e_g orbitals of $\text{LaCo}_{0.5}\text{Ni}_{0.5}\text{O}_3$ is larger than that of LaCoO_3 . The presence of itinerant σ^* electrons and t_{2g} holes was proposed as necessary conditions to show the ferromagnetism not only in $\text{LaCo}_{1-x}\text{Ni}_x\text{O}_3$ but also in $\text{SrFe}_{1-x}\text{Co}_x\text{O}_3$, SrCoO_3 , and $\text{Sr}_{1-x}\text{La}_x\text{CoO}_3$.

DOI: 10.1103/PhysRevB.68.104416

PACS number(s): 75.30.-m, 75.40.Cx, 75.50.Dd

I. INTRODUCTION

Perovskite-type oxides, the chemical formula of which is ABO_3 , with transition-metal ions at the B site have been investigated in order to understand the interactions of d electrons in the BO_6 octahedra network connected by the apical oxygen atoms with a $\sim 180^\circ$ B - O - B bond angle. Particularly, the oxides with quarter-filled $3d$ - e_g orbitals have attracted much studies, because the degree of freedom to occupy one of the twofold-degenerate e_g orbitals is connected with some interesting physical properties, such as the Jahn-Teller effect, orbital ordering, metallicity, and ferromagnetism.

The $t_{2g}^3e_g^1$ system has been widely investigated for an insulating LaMnO_3 .¹⁻⁶ The cooperative Jahn-Teller effect occurs at around 750 K accompanied by the characteristic ordering of occupied d_{x^2} and d_{y^2} orbitals.² The Curie-Weiss temperature of LaMnO_3 is positive in spite of the antiferromagnetic ground state,^{1,2} which has been understood by the anisotropic superexchange interaction due to the orbital ordering; ferromagnetic layers are coupled antiferromagnetically. Zhou *et al.* suggested that a long-range ferromagnetic order appears when the occupied e_g orbitals are arranged in a disordered fashion as demonstrated in $\text{LaMn}_{1-x}\text{Ga}_x\text{O}_3$.³ It is well known that the real charge transfer between Mn^{3+} and Mn^{4+} ions induces ferromagnetism and metallicity based on the double-exchange mechanism when holes are introduced into e_g orbitals, such as $\text{La}_{1-x}\text{Sr}_x\text{MnO}_3$.⁴⁻⁶ Zhou *et al.* also suggested that the double-exchange interaction acts even in nondoped LaMnO_3 above the orbital ordering temperature.²

A metallic SrFeO_3 has been investigated as another $t_{2g}^3e_g^1$ system.⁷⁻¹⁰ The Curie-Weiss temperature of SrFeO_3 is also positive in spite of the helical antiferromagnetic ground state,⁹ which has been understood by the coexistence of a nearest-neighbor ferromagnetic interaction and long-range antiferromagnetic interaction. In spite of the quarter-filled e_g orbitals, SrFeO_3 does not show Jahn-Teller distortion, which

has been understood by the itinerant nature of e_g electrons accommodated in a σ^* band formed between Fe e_g and O $2p$ orbitals or by the ground state dominated by a d^5L configuration instead of a d^4 configuration, where L is the oxygen hole state.^{10,23} The $t_{2g}^6e_g^1$ system has been investigated for LNiO_3 (L , rare-earth element).¹¹⁻¹⁶ LaNiO_3 is a metallic Pauli paramagnet with enhanced magnetic susceptibility.¹¹⁻¹³ No Jahn-Teller distortion exists in LaNiO_3 . The other LNiO_3 are insulating antiferromagnets with a complex spin arrangement.¹⁴⁻¹⁶ Though the deformation parameter of NiO_6 octahedra (defined as the standard deviation of six Ni-O bond lengths) increases as the size of L^{3+} ions decreases in the insulating LNiO_3 , the deformation parameter is about 30 times smaller than that of LaMnO_3 .¹⁶ Recently, Potze *et al.* suggested that trivalent and tetravalent Co ions are other candidates for the ion with quarter-filled e_g orbitals in spite of their $3d^6$ and $3d^5$ configurations,¹⁷ which is connected with the ferromagnetism in SrCoO_3 .¹⁸ The electronic configurations having one e_g electron and t_{2g} holes, $t_{2g}^5e_g^1$ and $t_{2g}^4e_g^1$, are termed as an intermediate-spin state. In addition to SrCoO_3 ,¹⁷⁻¹⁹ solid solutions including Co ions, $\text{SrFe}_{1-x}\text{Co}_x\text{O}_3$,²⁰⁻²³ $\text{Sr}_{1-x}\text{La}_x\text{CoO}_3$,²⁴⁻²⁶ and $\text{LaCo}_{1-x}\text{Ni}_x\text{O}_3$,²⁷⁻³² show metallicity and ferromagnetism in a certain x range.

It has been considered that the small or negative charge transfer energy from oxygen to transition-metal ions is important for the metallicity in the above oxides SrFeO_3 , $\text{SrFe}_{1-x}\text{Co}_x\text{O}_3$, SrCoO_3 , $\text{Sr}_{1-x}\text{La}_x\text{CoO}_3$, $\text{LaCo}_{1-x}\text{Ni}_x\text{O}_3$, and LaNiO_3 , because the $3d$ level of highly oxidized transition-metal ions, such as Fe^{4+} , Co^{4+} , Co^{3+} , and Ni^{3+} , is deep and close to the O^{2-} $2p$ level. However, the origin of the magnetic interaction in these metallic oxides has not yet been clarified as compared to manganese oxides. The metallic oxides including Co ions show ferromagnetism, in spite of the different number of $3d$ electrons between 4 and 7. Thus, the clarification of the relation of ferromagnetism to

the presence or absence, valence, and spin state of Co ions should provide a clue to understand the origin of magnetic interaction in the metallic oxides. The present study investigated $\text{LaCo}_{0.5}\text{Ni}_{0.5}\text{O}_3$ because of the lack of systematic studies regarding it, particularly valence and spin states. In addition, we discuss the origin of the ferromagnetism appearing in the metallic oxides with $3d$ electrons between 4 and 7.

II. EXPERIMENT

$\text{LaCoO}_{3-\delta}$ and $\text{LaCo}_{0.5}\text{Ni}_{0.5}\text{O}_{3-\delta}$ were prepared by a solid-state reaction method from La_2O_3 , NiO , and $\text{CoC}_2\text{O}_4 \cdot 2\text{H}_2\text{O}$. The mixed powder was calcined in air at 1273–1473 K, pressed into pellets, and sintered in air at 1473–1573 K for 12 h. $\text{LaNiO}_{3-\delta}$ was prepared by a precursor method using citric acid from La_2O_3 and Ni . The precursor was fired at 1073 K for 24 h. Iodometric titration and thermogravimetric analyses determined the oxygen deficiency, -0.02 , -0.01 , and 0.1 within the experimental error ± 0.02 for $\text{LaCoO}_{3-\delta}$, $\text{LaCo}_{0.5}\text{Ni}_{0.5}\text{O}_{3-\delta}$, and $\text{LaNiO}_{3-\delta}$, respectively. The prepared $\text{LaCoO}_{3-\delta}$ and $\text{LaNiO}_{3-\delta}$ and commercial CoO and NiO were used for the references of x-ray-absorption near-edge structure (XANES).

Powder x-ray diffraction (XRD) measurements using $\text{Cu } K\alpha$ radiation (MAC Science, MXP18HF) clarified that the samples are single phase with a rhombohedral unit cell. All the detected diffraction peaks were consistent with the space group $R\bar{3}c$. Lattice parameters of $\text{LaCo}_{0.5}\text{Ni}_{0.5}\text{O}_3$ and LaNiO_3 were determined in air in the range 27–1220 K and 420–1220 K, respectively, from some high-angle diffraction peaks using Si crystalline powder as an internal standard. The XRD pattern and the lattice parameters at room temperature did not change before and after the sample was heated to 1220 K. This indicates neither appreciable oxidation of Si nor chemical reaction of Si with the sample up to 1220 K during the measurement period. Structural parameters of LaNiO_3 , $\text{LaCo}_{0.5}\text{Ni}_{0.5}\text{O}_3$, and LaCoO_3 at around 30 K were determined by Rietveld refinements using RIETAN-2000.³³ XANES was measured at room temperature (RIGAKU, R-XAS Looper). dc magnetizations were measured using a superconducting quantum interference device (SQUID) magnetometer (Quantum Design, MPMS5S) in the range 5–300 K and using a magnetic balance (Shimadzu, MB-1A) in the range 300–1100 K. ac magnetic susceptibilities, dc resistivities, and heat capacities were measured in the range 2–200 K (Quantum Design, PPMS). Thermogravimetric analysis was carried out in the range 300–1273 K (MAC Science, 2000S).

III. RESULTS

Figures 1(a) and 1(b) show Co K -edge and Ni K -edge XANES, respectively, at room temperature. The Co K and the Ni K absorption edges of $\text{LaCo}_{0.5}\text{Ni}_{0.5}\text{O}_3$ are close to those of LaCoO_3 and LaNiO_3 and clearly higher than those of CoO and NiO , respectively. It concludes that both valences of Co and Ni ions in $\text{LaCo}_{0.5}\text{Ni}_{0.5}\text{O}_3$ are trivalent at least at room temperature.

Structural parameters at around 30 K determined by

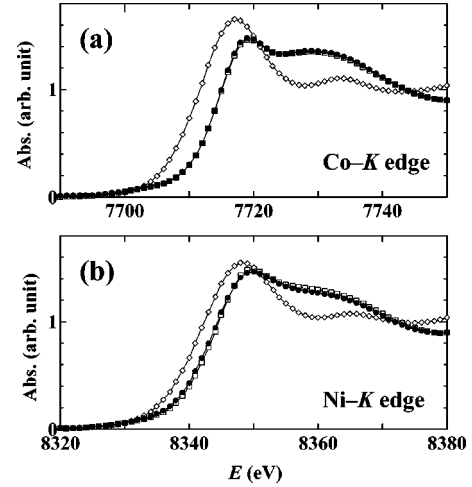


FIG. 1. (a) Co K -edge XANES: \bullet , $\text{LaCo}_{0.5}\text{Ni}_{0.5}\text{O}_3$; \square , LaCoO_3 ; \diamond , CoO . (b) Ni K -edge XANES: \bullet , $\text{LaCo}_{0.5}\text{Ni}_{0.5}\text{O}_3$; \square , LaNiO_3 ; \diamond , NiO .

Rietveld refinements and reliability factors for the fitting are tabulated in Table I. The composition x dependence of the unit-cell volume, B -O bond length, and B -O- B bond angle of $\text{LaCo}_{1-x}\text{Ni}_x\text{O}_3$ ($B = \text{Co}, \text{Ni}$) are shown in Figs. 2(a), 2(b), and 2(c), respectively. The literature values (open circles) determined by neutron diffraction are plotted for LaCoO_3 at 31 K (Ref. 34) and LaNiO_3 at 30 K (Ref. 14) together with the present data (solid circles). (The literature values of LaCoO_3 at 31 K were estimated by interpolating the data at 4 and 71 K.) The present data are coincident with the literature data within the fitting error, which ensures the accuracy of the present data. The unit cell volume and the B -O bond length are largest and the B -O- B bond angle is smallest at $x = 0.5$. The largest B -O bond length at $x = 0.5$ indicates that the average size of B -site ions in $\text{LaCo}_{0.5}\text{Ni}_{0.5}\text{O}_3$ is larger than that of either Co ions in LaCoO_3 or Ni ions in LaNiO_3 . In addition, the B -O- B bond angle being smallest at $x = 0.5$ is also understood by the decreased tolerance factor $t = (r_{\text{La}^{3+}} + r_{\text{O}^{2-}}) / \sqrt{2}(r_{\text{B}^{3+}} + r_{\text{O}^{2-}})$, which increases the tilt angle of the BO_6 octahedron, where r_M is the radius of the M ion.

Figure 3(a) shows the temperature dependence of the unit-

TABLE I. Structural parameters of $\text{LaCo}_{1-x}\text{Ni}_x\text{O}_3$ determined by Rietveld refinement with the space group $R\bar{3}c$. Isotropic temperature factors of La, B (= Co, Ni), and O were fixed at 0.1, 0.1, and 0.2, respectively.

x	0	0.5	1
T (K)	31	27	33
a (\AA)	5.4250(5)	5.4620(6)	5.451(2)
c (\AA)	13.0065(8)	13.077(1)	13.115(2)
V (\AA^3)	331.51(5)	337.86(6)	337.4(1)
$x[\text{O}]$	0.5529(6)	0.5543(5)	0.5462(6)
$d_{\text{B-O}}$ (\AA)	1.9260(7)	1.9394(6)	1.9323(9)
$\theta_{\text{B-O-B}}$ (deg)	162.9(2)	162.5(2)	165.0(2)
R_{wp} (%)	13.15	10.75	10.41
R_I (%)	3.82	5.83	1.37

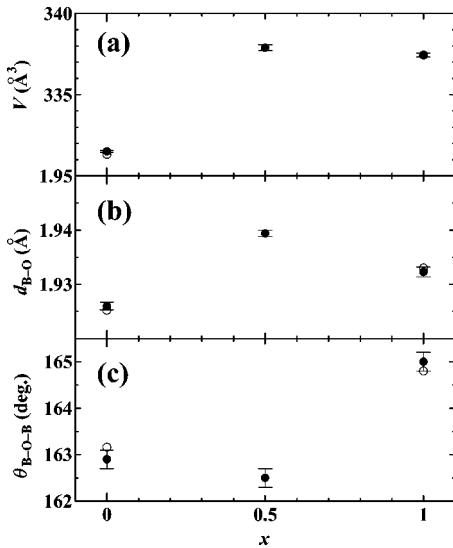


FIG. 2. Composition dependences of (a) unit-cell volume, (b) B-O bond length, and (c) B-O-B bond angle of $\text{LaCo}_{1-x}\text{Ni}_x\text{O}_3$ around 30 K: \bullet , present data (Table I); \circ , literature data (Refs. 14 and 34).

cell volume of $\text{LaCo}_{0.5}\text{Ni}_{0.5}\text{O}_3$, LaCoO_3 ,³⁴ and LaNiO_3 .¹⁴ Thermogravimetric analysis of $\text{LaCo}_{0.5}\text{Ni}_{0.5}\text{O}_3$ confirmed that the evolution of oxygen from the sample is at most $\delta = 0.01$ between room temperature and 1273 K. The thermal expansion of LaCoO_3 between 0 and ~ 1200 K is about twice as large as that of LaNiO_3 . The large thermal expansion of LaCoO_3 has been attributed to the spin-state transition of trivalent Co ions from the low-spin state to the high- or intermediate-spin state.³⁵ The thermal expansion and the unit-cell volume of $\text{LaCo}_{0.5}\text{Ni}_{0.5}\text{O}_3$ are very close to those of LaNiO_3 below room temperature. This implies that the spin state (and the valence) does not change appreciably below room temperature. The thermal expansion of $\text{LaCo}_{0.5}\text{Ni}_{0.5}\text{O}_3$

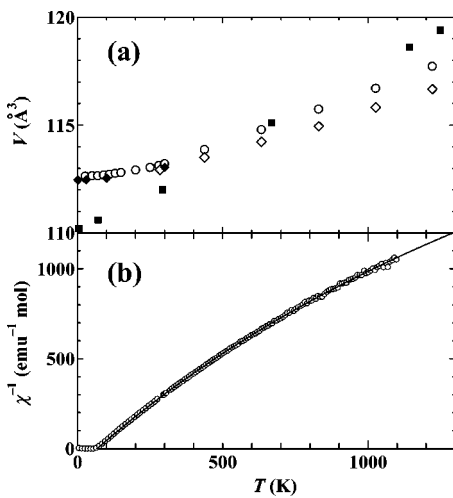


FIG. 3. (a) Temperature dependences of the unit-cell volume: \circ , $\text{LaCo}_{0.5}\text{Ni}_{0.5}\text{O}_3$ (present data); \diamond , LaNiO_3 (present data); \blacksquare , LaCoO_3 (Ref. 34); \blacklozenge , LaNiO_3 (Ref. 14). (b) Temperature dependence of the reciprocal magnetic susceptibility of $\text{LaCo}_{0.5}\text{Ni}_{0.5}\text{O}_3$. A solid line is the result of fitting using Eq. (1).

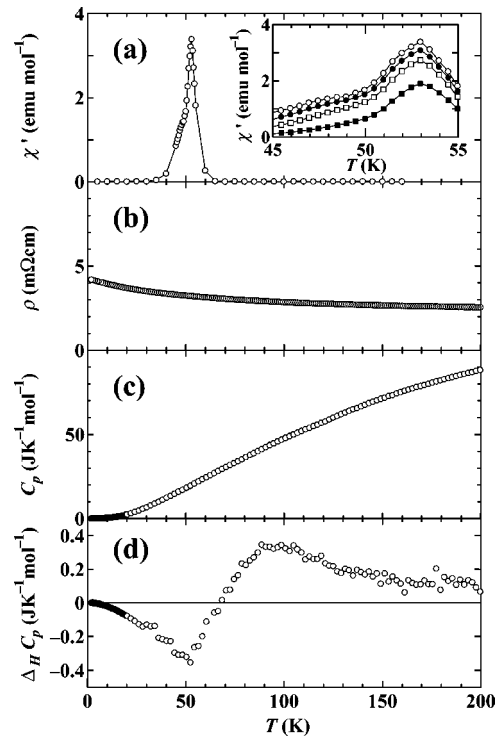


FIG. 4. (a) Real parts of the ac magnetic susceptibility: \circ , 10 Hz; \bullet , 100 Hz; \square , 1 kHz; \blacksquare , 10 kHz, (b) resistivity, (c) heat capacity: \circ , 0 Oe; \bullet , 90 kOe, and (d) $\Delta_H C_p = C_p(90 \text{ kOe}) - C_p(0 \text{ Oe})$ of $\text{LaCo}_{0.5}\text{Ni}_{0.5}\text{O}_3$.

becomes larger than that of LaNiO_3 above room temperature and the unit-cell volume is between those of LaCoO_3 and LaNiO_3 above 600 K.

Figure 3(b) shows the temperature dependence of the reciprocal magnetic susceptibility of $\text{LaCo}_{0.5}\text{Ni}_{0.5}\text{O}_3$. The temperature-independent diamagnetic contribution due to the core electrons, $-6.58 \times 10^{-5} \text{ emu mol}^{-1}$, has already been subtracted from the raw data. The upward convex $\chi^{-1}-T$ curve was well reproduced by the equation

$$\chi = \frac{C}{T - \theta} + \chi_0 \quad (1)$$

as indicated by the solid line in the figure which was obtained by the least-squares fitting of the data above 100 K. The best-fit parameters are $C = 0.71(4) \text{ emu mol}^{-1} \text{ K}$ [corresponding to $\mu_{\text{eff}} = 2.4(1) \mu_B$], $\theta = 67(4) \text{ K}$, and $\chi_0 = 2.6(1) \times 10^{-4} \text{ emu mol}^{-1}$. Vasanthacharya *et al.* have suggested the ferrimagnetic ordering in $\text{LaCo}_{0.5}\text{Ni}_{0.5}\text{O}_3$ based on the upward convex character of $\chi^{-1}-T$ curve.²⁸ However, the fact that the $\chi^{-1}-T$ curve is well reproduced by Eq. (1) in a wide temperature range would reject this suggestion, because the $\chi^{-1}-T$ curve of a ferrimagnet should show a sudden bending as the temperature approaches the ordering temperature.

Figure 4(a) shows real parts of the ac magnetic susceptibility of $\text{LaCo}_{0.5}\text{Ni}_{0.5}\text{O}_3$ at 10 Hz. The inset shows the frequency dependence in the temperature range 45–55 K. A peak and a shoulder were observed at 53 K and around 48 K,

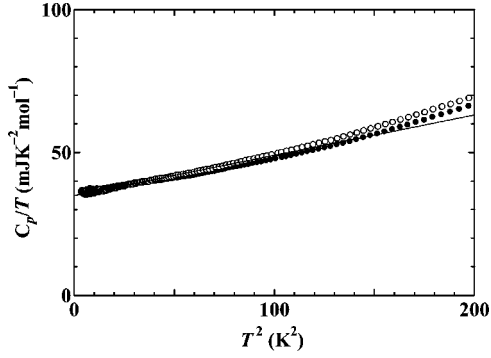


FIG. 5. C_p/T vs T^2 plot of $\text{LaCo}_{0.5}\text{Ni}_{0.5}\text{O}_3$: \circ , 0 Oe; \bullet , 90 kOe. A solid line is the result of fitting using Eq. (2).

respectively. The peak temperature does not appreciably depend on the frequency while the peak magnitude depends on the frequency. The resistivity shown in Fig. 4(b) is on the order of $10^{-3} \Omega \text{ cm}$ and slightly increases with decreasing temperature, having a temperature derivative much smaller than that of a semiconductor. No appreciable anomaly was observed in the resistivity around 50 K. The open and solid circles in Fig. 4(c) represent heat capacities of $\text{LaCo}_{0.5}\text{Ni}_{0.5}\text{O}_3$ under 0 and 90 kOe, respectively. Because of the similar value, the data are superimposed. Figure 4(d) shows $\Delta_H C_p = C_p(90 \text{ kOe}) - C_p(0 \text{ Oe})$, where $C_p(H)$ is the heat capacity measured under a magnetic field H . A clear cusp was observed in $\Delta_H C_p$ at around 53 K corresponding to the peak in ac magnetic susceptibility. In addition to this, the absence of an appreciable frequency dependence in the ac susceptibility peak temperature suggests the presence of a critical ferromagnetic ordering temperature at 53 K. On the other hand, no appreciable anomaly was observed around 48 K corresponding to the shoulder seen in the ac magnetic susceptibility. In the light of the lack of a connection between the entropy and shoulder, the magnetic anomaly around 48 K might be connected to the freezing of magnetic domains.

Open and solid circles in Fig. 5 represent the C_p/T vs T^2 plot of $\text{LaCo}_{0.5}\text{Ni}_{0.5}\text{O}_3$ under 0 and 90 kOe, respectively. No appreciable difference was observed below $\sim 7 \text{ K}$ between 0 and 90 kOe. This implies that the contribution from the ferromagnetic spin-wave excitation is small even if present possibly because of the large energy gap. Therefore, the low-temperature heat capacity is expressed by

$$C_p = \gamma T + \beta T^3. \quad (2)$$

The best-fit parameters obtained from the data below 7 K under zero field are $\gamma = 34.9(7) \text{ mJ K}^{-2} \text{ mol}^{-1}$ and $\beta = 0.141(3) \text{ mJ K}^{-4} \text{ mol}^{-1}$. The magnitudes of γ and β are similar to those of a metallic ferromagnet $\text{La}_{1-x}\text{Sr}_x\text{CoO}_3$,²⁶ but smaller than that of LaNiO_3 .¹² The magnitude of resistivity was on the order of metal while the temperature derivative of the resistivity was negative as shown in Fig. 4(b). The presence of electronic specific heat clarified the metallicity. This is the same conclusion as that of the literature.²⁹

Figure 6 shows the M vs H plot at 5 K measured after zero-field cooling. The magnetization does not saturate even

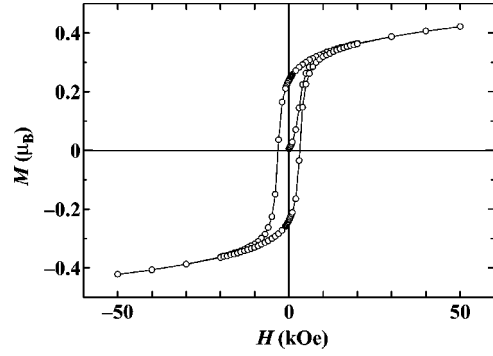


FIG. 6. M vs H plot of $\text{LaCo}_{0.5}\text{Ni}_{0.5}\text{O}_3$ at 5 K.

at 50 kOe. Taking account of this, the shoulder in ac susceptibility around 48 K, and the small heat capacity anomaly at 53 K, the presence of a glasslike component is supposed as suggested by Asai *et al.*²⁷ However, the reverse of magnetization at the coercive force around $\pm 5 \text{ kOe}$ is relatively sharp as compared to a spin-glass system. This implies the presence of ferromagnetic domains large enough to include domain walls, even if a glasslike component coexists. The magnetization at 50 kOe is much smaller than the effective magnetic moment $2.4 \mu_B$ estimated by Eq. (1).

IV. DISCUSSION

XANES and the unit-cell volume clarified that a 1:1 solid solution of LaCoO_3 and LaNiO_3 leaves the valences of Co and Ni ions trivalent but expands the average $B\text{-O}$ bond length from the average of Co-O bond length in LaCoO_3 and Ni-O bond length in LaNiO_3 . It is thus considered that the solid solution increased the population of e_g orbitals of Co or Ni ions (or σ^* band) from those of LaCoO_3 ($t_{2g}^6 e_g^0$) or LaNiO_3 ($t_{2g}^6 e_g^1$). We have reported that the spin state of Co ions in LaCoO_3 is sensitive to the substitution of Co by another trivalent M ion.³⁶ In addition, only a low-spin state has been reported for the trivalent Ni ions in perovskite-type oxides as far as we know. Therefore, it is natural to consider that the solid solution changes the spin state of Co ions and leaves the spin state of Ni ions at the low-spin state. This consideration is consistent with our suggestion in the earlier paper:³⁶ The low-spin state of Co ions in LaCoO_3 is destabilized (stabilized) as compared to the high- or intermediate-spin state when the Co ions are substituted by trivalent M ions with Pauling electronegativity larger (smaller) than that of the Co atom. Considering that Pauling electronegativity increases with the increase in the atomic number from Ti to Cu,³⁷ the Pauling electronegativity of Ni atoms would be larger than that of Co atoms, though the same values are tabulated for Co and Ni atoms in Pauling's table. Therefore, the substitution of Co^{3+} in LaCoO_3 by Ni^{3+} should increase the population of trivalent Co e_g orbitals.

It is difficult to determine the electronic configuration of Co ions in $\text{LaCo}_{0.5}\text{Ni}_{0.5}\text{O}_3$ using the Curie constant, because it is unclear whether the localized picture correctly depicts the ferromagnetism, and the origin of the large χ_0 is undetermined. However, it was found that the unit-cell volume of $\text{LaCo}_{0.5}\text{Ni}_{0.5}\text{O}_3$ is close to (slightly larger than) that of

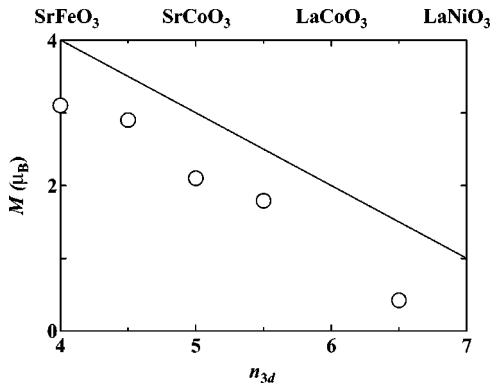


FIG. 7. Magnetization at a high field and a low temperature (open circles) for SrFe_{0.5}Co_{0.5}O₃, SrCoO₃, Sr_{0.5}La_{0.5}CoO₃, and LaCo_{0.5}Ni_{0.5}O₃ and the Fe magnetic moment for SrFeO₃ estimated by neutron diffraction as a function of the number of 3d electrons, n_{3d} . A solid line represents the theoretical magnetization expected from the $t_{2g}^{n_{3d}-1}\sigma^{*1}$ configuration and the full spin polarizations.

LaNiO₃ below room temperature. This result indicates that the size of Co ions is similar to that of the low-spin trivalent Ni ion. This rejects at least a possibility of the high-spin state of Co ions, because the ion radius is much larger than that of the low-spin trivalent Ni ion.³⁸ The intermediate-spin state with $t_{2g}^5e_g^1$ configuration might be consistent with this result, because the population of e_g orbitals is the same as that of the low-spin trivalent Ni ion, which may give a similar size. The long-range configuration of Ni and Co ions in LaCo_{0.5}Ni_{0.5}O₃ would be disordered due to their similar ion sizes. This must be a reason for the glasslike component observed in the present study.

Kobayashi *et al.* have reported that the magnetic and transport properties of LaCo_{1-x}Ni_xO₃ are similar to those of La_{1-x}Sr_xCoO₃, at least in the La-rich region.³⁹ They suggested that the substitution of Co by Ni induces a charge transfer from Co³⁺ to Ni³⁺, resulting in Co⁴⁺ and Ni²⁺. However, the present study clarified that such a charge transfer does not occur at least at $x=0.5$. Instead, the present study suggested that the Ni substitution increases the population of Co e_g orbitals as stated above. The same population change has been suggested for La_{1-x}Sr_xCoO₃ with increasing x .²⁶ In addition, the present study clarified that the anomalously large electronic specific heat coefficient of LaCo_{0.5}Ni_{0.5}O₃ is comparable to that of La_{1-x}Sr_xCoO₃. These results suggest that the structure of the σ^* band and the electronic state, such as the population, density of states at Fermi level, and the electron correlation, are essentially same between LaCo_{1-x}Ni_xO₃ and La_{1-x}Sr_xCoO₃.

As mentioned in Sec. I, the quarter-filled σ^* band is expected for the electronic structure of SrFeO₃, SrFe_{1-x}Co_xO₃, SrCoO₃, Sr_{1-x}La_xCoO₃, LaCo_{1-x}Ni_xO₃, and LaNiO₃. The open circles in Fig. 7 represent the experimental magnetization at a high field and a low temperature for SrFe_{0.5}Co_{0.5}O₃,²² SrCoO₃,¹⁸ Sr_{0.5}La_{0.5}CoO₃,²⁵ and LaCo_{0.5}Ni_{0.5}O₃ and the magnetic moment of Fe ions in SrFeO₃ estimated by neutron diffraction experiment^{9,10} as a function of the number of 3d electrons, n_{3d} . The solid line in the figure indicates the theoretical magnetization expected

from the $t_{2g}^{n_{3d}-1}\sigma^{*1}$ configuration and the full spin polarizations. The experimental and theoretical magnetizations seem to decrease at a common rate with increasing n_{3d} . This implies that the electrons occupy the minor-spin t_{2g} orbitals instead of the major-spin σ^* band above $n_{3d}=4$. However, the experimental magnetization is about $1\mu_B$ smaller than the theoretical one in each sample. Two possibilities are supposed for the reason why the magnetization at a high field and a low temperature is smaller than the theoretical one. One is that the polarization is incomplete and the other is that some antiferromagnetic interaction coexists with a ferromagnetic one. The latter might be plausible for LaCo_{0.5}Ni_{0.5}O₃, because a glasslike component was observed as expected from the chemical disorder at the B site. On the other hand, the latter is not plausible for SrFeO₃ and SrCoO₃, because chemical disorder is absent. It is thus difficult to conclude which possibility is essential for these metallic materials. This will be clarified by investigating the spin arrangement of each ion using methods such as an x-ray magnetic circular dichroism (XMCD) technique.

The present study clarified that the valence of Co ions is not important for SrFe_{1-x}Co_xO₃, Sr_{1-x}La_xCoO₃, and LaCo_{1-x}Ni_xO₃ showing ferromagnetism, because these oxides formally include only tetravalent, both tetravalent and trivalent, and only trivalent Co ions, respectively. In addition, taking account of the fact that SrFeO₃ is essentially a ferromagnet, the presence or absence of Co ions would not be very important for the ferromagnetism. We propose two necessary conditions for the ferromagnetism, t_{2g} holes and itinerant σ^* electrons, based on the following three facts. (1) Though LaCo_{0.5}Ni_{0.5}O₃ shows metallicity and ferromagnetism, NdCo_{0.5}Ni_{0.5}O₃ shows insulating and spin-glass behaviors.^{40,41} In addition, x of the unit-cell volume of NdCo_{1-x}Ni_xO₃ shows a linear dependence,⁴¹ which indicates that most Co and Ni ions remain in their low-spin trivalent states. These facts imply a connection among the ferromagnetism, metallicity (itinerant σ^* electrons), and/or t_{2g} holes. (2) LaNiO₃ shows no ferromagnetism, which implies a connection between the ferromagnetism and t_{2g} holes. (3) LaCo_{0.5}Rh_{0.5}O₃ shows neither metallicity nor ferromagnetism although most trivalent Co ions are not in the low-spin state,³⁶ which implies a connection between ferromagnetism and metallicity (itinerant σ^* electrons).

V. CONCLUDING REMARKS

In conclusion, the present study clarified that a 1:1 solid solution of LaCoO₃ and LaNiO₃ leaves the valences of Co and Ni ions trivalent and suggested that the solid solution increases the population of trivalent Co e_g orbitals from $t_{2g}^6e_g^0$ in LaCoO₃. In addition, it was proposed that the electronic configuration of metallic oxides SrFeO₃, SrFe_{1-x}Co_xO₃, SrCoO₃, Sr_{1-x}La_xCoO₃, LaCo_{1-x}Ni_xO₃, and LaNiO₃ is $t_{2g}^{n_{3d}-1}\sigma^{*1}$ and that t_{2g} holes and itinerant σ^* electrons are necessary for the ferromagnetism. The ferromagnetism might originate from a double-exchange interaction similar to La_{1-x}Sr_xMnO₃.⁴⁻⁶ However, the long-range antiferromagnetic interaction present in SrFeO₃ (Ref. 9) is different from the characters of La_{1-x}Sr_xMnO₃. This inter-

action should be considered carefully in order to clarify whether or not the origin of ferromagnetism is a double-exchange interaction.

Though $\text{LaCo}_{0.5}\text{Ni}_{0.5}\text{O}_3$ is considered to be essentially a metallic ferromagnet, there remain many unresolved issues: these include the origin of large χ_0 and large γ , the fact that the magnetization does not saturate even at 50 kOe and at 5 K, and the reason why the magnetization at 50 kOe is much smaller than the effective magnetic moment. These problems

should be clarified in connection with the electronic structure, ferromagnetic domain structure (including glasslike component), and chemical order and disorder.

ACKNOWLEDGMENT

Part of this work was financially supported by a Grant-in-Aid for Scientific Research from the Ministry of Education, Science, Culture, and Sports of Japan.

- *Author to whom correspondence should be addressed. Electronic address: Mitsuru_Itoh@msl.titech.ac.jp
- ¹G.H. Jonker, *Physica (Amsterdam)* **22**, 707 (1956).
 - ²J.-S. Zhou and J.B. Goodenough, *Phys. Rev. B* **60**, R15 002 (1999).
 - ³J.-S. Zhou, H.Q. Yin, and J.B. Goodenough, *Phys. Rev. B* **63**, 184423 (2001).
 - ⁴C. Zener, *Phys. Rev.* **82**, 403 (1951).
 - ⁵P.W. Anderson and H. Hasagawa, *Phys. Rev.* **100**, 675 (1955).
 - ⁶P.G. de Gennes, *Phys. Rev.* **118**, 141 (1960).
 - ⁷P.K. Gallagher, J.B. MacChesney, and D.N.E. Buchanan, *J. Chem. Phys.* **41**, 2429 (1964).
 - ⁸J.B. MacChesney, R.C. Sherwood, and J.F. Poter, *J. Chem. Phys.* **43**, 1907 (1965).
 - ⁹T. Takeda, Y. Yamaguchi, and H. Watanabe, *J. Phys. Soc. Jpn.* **33**, 967 (1972).
 - ¹⁰A.E. Bocquet, A. Fujimori, T. Mizokawa, T. Saitoh, H. Namatame, N. Kimizuka, Y. Takeda, and M. Takano, *Phys. Rev. B* **45**, 1561 (1992).
 - ¹¹J.B. Goodenough, N.F. Mott, M. Pouchard, G. Demazeau, and P. Hagenmuller, *Mater. Res. Bull.* **8**, 647 (1973).
 - ¹²K. Sreedhar, J.M. Honig, M. Darwin, M. McElfresh, P.M. Shand, J. Xu, B.C. Crooker, and J. Spalek, *Phys. Rev. B* **46**, 6382 (1992).
 - ¹³J.-S. Zhou, J.B. Goodenough, B. Dabrowski, P.W. Klamut, and Z. Bukowski, *Phys. Rev. Lett.* **84**, 526 (2000).
 - ¹⁴J.L. García-Muñoz, J. Rodríguez-Carvajal, P. Lacorre, and J.B. Torrance, *Phys. Rev. B* **46**, 4414 (1992).
 - ¹⁵J.L. García-Muñoz, J. Rodríguez-Carvajal, and P. Lacorre, *Phys. Rev. B* **50**, 978 (1994).
 - ¹⁶J.A. Alonso, M.J. Marínez-Lope, M.T. Casais, J.L. García-Muñoz, and M.T. Fernández-Díaz, *Phys. Rev. B* **61**, 1756 (2000).
 - ¹⁷R.H. Potze, G.A. Sawatzky, and M. Abbate, *Phys. Rev. B* **51**, 11 501 (1995).
 - ¹⁸P. Bezdzicka, A. Wattiaux, J.C. Grenier, M. Pouchard, and P. Hagenmuller, *Z. Anorg. Allg. Chem.* **619**, 7 (1993).
 - ¹⁹Y. Takeda, R. Kanno, T. Takada, O. Yamamoto, M. Takano, and Y. Bando, *Z. Anorg. Allg. Chem.* **540/541**, 259 (1986).
 - ²⁰T. Takeda and H. Watanabe, *J. Phys. Soc. Jpn.* **33**, 973 (1972).
 - ²¹P. Bezdzicka, L. Fournes, A. Wattiaux, J.C. Grenier, and M. Pouchard, *Solid State Commun.* **91**, 501 (1994).
 - ²²S. Kawasaki, M. Takano, and Y. Takeda, *J. Solid State Chem.* **121**, 174 (1996).
 - ²³M. Abbate, G. Zampieri, J. Okamoto, A. Fujimori, S. Kawasaki, and M. Takano, *Phys. Rev. B* **65**, 165120 (2002).
 - ²⁴M. Itoh, I. Natori, I. Kubota, and M. Motoya, *J. Phys. Soc. Jpn.* **63**, 1486 (1994).
 - ²⁵M.A. Señaris-Rodríguez and J.B. Goodenough, *J. Solid State Chem.* **118**, 323 (1995).
 - ²⁶S. Tsubouchi, T. Kyômen, and M. Itoh, *Phys. Rev. B* **67**, 094437 (2003).
 - ²⁷K. Asai, H. Sekizawa, K. Mizushima, and S. Iida, *J. Phys. Soc. Jpn.* **43**, 1093 (1977).
 - ²⁸N.Y. Vasantharya, P. Ganguly, and C.N.R. Rao, *J. Solid State Chem.* **53**, 140 (1984).
 - ²⁹K.P. Rajeev and A.K. Raychaudhuri, *Phys. Rev. B* **46**, 1309 (1992).
 - ³⁰H. Sawada, N. Hamada, and K. Terakura, *J. Phys. Chem. Solids* **56**, 1755 (1995).
 - ³¹J. Pérez, J. García, J. Blasco, and J. Stankiewicz, *Phys. Rev. Lett.* **80**, 2401 (1998).
 - ³²M.T. Escode, C.H. Westphal, and R.F. Jardim, *J. Appl. Phys.* **87**, 5908 (2000).
 - ³³F. Izumi and T. Ikeda, *Mater. Sci. Forum* **321-324**, 198 (2000).
 - ³⁴G. Thornton, B.C. Tofield, and A.W. Hewat, *J. Solid State Chem.* **61**, 301 (1986).
 - ³⁵K. Asai, A. Yoneda, O. Yokokura, J.M. Tranquada, G. Shirane, and K. Kohn, *J. Phys. Soc. Jpn.* **67**, 290 (1998).
 - ³⁶T. Kyômen, Y. Asaka, and M. Itoh, *Phys. Rev. B* **67**, 144424 (2003).
 - ³⁷L. Pauling, *The Nature of the Chemical Bond* (Cornell University Press, Ithaca, 1960).
 - ³⁸R.D. Shannon, *Acta Crystallogr., Sect. A: Cryst. Phys., Diffr., Theor. Gen. Crystallogr.* **32**, 751 (1976).
 - ³⁹Y. Kobayashi, S. Murata, K. Asai, J.M. Tranquada, G. Shirane, and K. Kohn, *J. Phys. Soc. Jpn.* **68**, 1011 (1999).
 - ⁴⁰J. Blasco and J. García, *J. Phys. Chem. Solids* **55**, 843 (1994).
 - ⁴¹J. Blasco and J. García, *Phys. Rev. B* **51**, 3569 (1995).